Pang *et al. Cardio-Oncology* (2025) 11:45
https://doi.org/10.1186/s40959-025-00342-5

Cardio-Oncology

RESEARCH Open Access

Development and validation of an early prediction model for cardiac death risk in patients with light chain amyloidosis: a multicenter study

Naidong Pang[1], Ying Tian[2,3], Hongjie Chi[1], Xiaohong Fu[4], Xin Li[5], Shuyu Wang[6], Feifei Pan[4], Dongying Wang[5], Lin Xu[1], Jingyi Luo[2,3], Aijun Liu[2,3*] and XingPeng Liu[1,7*]

Abstract

Background Cardiac involvement is the primary driver of death in systemic light chain (AL) amyloidosis. However, the early prediction of cardiac death risk in AL amyloidosis remains insufficient.

Objectives We aimed to develop a novel prediction model and prognostic scoring system that enables early identification of these high-risk individuals.

Methods This study enrolled 235 patients with confirmed AL cardiac amyloidosis from three hospitals. Patients from the first hospital were randomly assigned to the training and internal validation sets in an 8:2 ratio, while the external validation set comprised patients from the other two hospitals. Participants were categorized into a cardiac death group and a non-cardiac death group (including survivors and those who died from other causes). Five different machine learning models were used to train model, and model performance was evaluated using receiver operating characteristic (ROC) curves, calibration curves, and decision curve analysis.

Results All five models showed excellent performance on the training and internal validation sets. In external validation, both the Logistic Regression (LR) and Random Forest models achieved an area under the ROC curve of 0.873 and 0.877, respectively, and exhibited superior calibration and decision curve analysis. Considering the comprehensive performance and clinical applicability, the LR model was selected as the final prediction model. The visualization results are ultimately presented in a nomogram. Further analyses were performed on the newly identified predictors.

Conclusions This prediction model enables early identification and risk assessment of cardiac death in patients with AL amyloidosis, exhibiting considerable predictive ability.

*Correspondence:
Aijun Liu
laj0628@163.com
XingPeng Liu
xpliu71@vip.sina.com

Full list of author information is available at the end of the article

Graphical Abstract

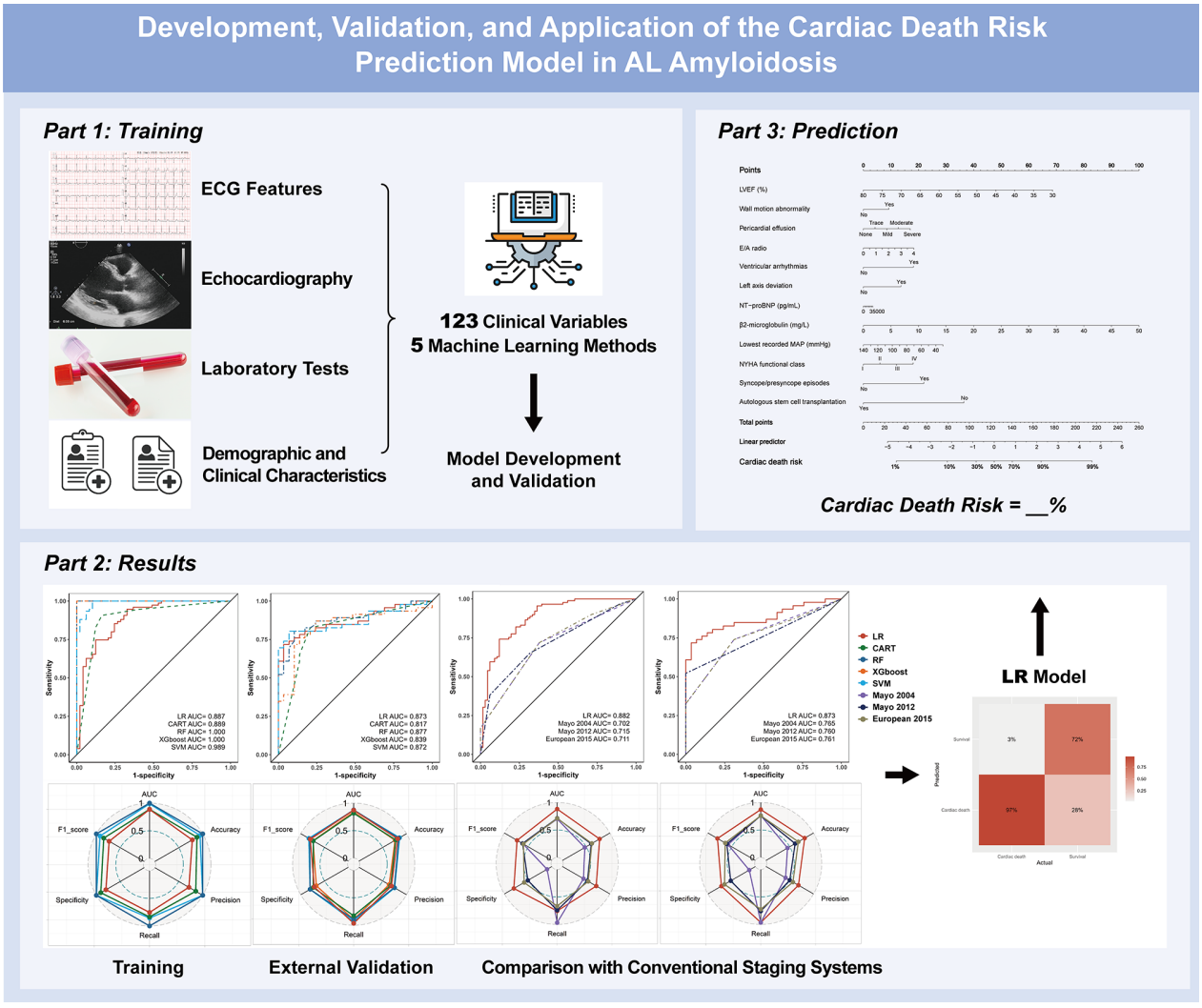

Keywords Light chain amyloidosis, Cardiac death, Sudden cardiac death, Machine learning, Prediction model, Nomogram

Introduction

Systemic light chain (AL) amyloidosis is characterized by the deposition of amyloid fibrils in various tissues and organs, leading to progressive organ dysfunction and failure, ultimately leading to death [1]. Cardiac involvement, present in over 75% of AL amyloidosis patients, is the primary driver of mortality [1–3]. Despite recent therapeutic advancements [4, 5], the prognosis for patients with advanced cardiac involvement remains poor, with a median survival of less than one year [6, 7].

Current survival estimation systems, such as the Mayo 2004 and 2012 staging systems, use cardiac troponin I (cTnI), N-terminal pro-brain natriuretic peptide (NT-proBNP), and the difference between involved and uninvolved free light chain levels for risk stratification [8, 9]. Several studies have refined and developed the Mayo staging system, primarily used for overall prognostic staging or renal outcome staging for AL amyloidosis, with a main emphasis on cardiac or multi-organ failure [10–13]. Although these systems are useful, they do not fully account for treatment protocols, changes in cardiac structure and function, and deaths related to sudden cardiac events [14]. As a result, high-risk patients, particularly those prone to sudden cardiac death and deaths related to malignant arrhythmias, often remain unrecognized in the early stages [15, 16].

This study aims to assess the risk of cardiac death in AL amyloidosis patients, focusing on worsening heart failure

(HF), sudden cardiac death, and malignant arrhythmias. Machine learning techniques are employed to develop a novel model and scoring system that predict the risk of cardiac death based on clinical characteristics at the first hospitalization, facilitating early identification of high-risk individuals.

Methods

Study population and design

This retrospective, observational, multicenter study included 235 patients diagnosed with AL cardiac amyloidosis from three hospitals across China. Patients were recruited consecutively from Beijing Chaoyang Hospital (Hospital A; $n = 157$; January 2014 to May 2023) and from the First and Second Hospitals of Shanxi Medical University (Hospitals B and C; $n = 78$; January 2019 to May 2023). Data from Hospital A were utilized for model development, with an 8:2 split between the training and internal validation sets. Patients from Hospitals B and C served as external validation cohorts. The study adhered to the Declaration of Helsinki and was approved by the Institutional Review Board of Beijing Chaoyang Hospital, with written informed consent obtained from all participants.

Inclusion criteria: (1) Age ≥ 18 years; (2) Diagnosis of AL amyloidosis with cardiac involvement based on international consensus criteria [17, 18]; (3) Availability of comprehensive medical records.

Exclusion criteria: (1) Significant incompleteness of baseline data, defined as more than 10% of variables missing; (2) Follow-up duration of less than 1 year.

Data extraction, follow-up, and definition of mode of death

Comprehensive clinical data for all patients were collected for machine learning feature extraction. In order to emphasize the early prediction capabilities of this model, all data were collected during initial hospitalization.

Patients were followed up for at least 12 months, from April to May 2024, via telephone or clinic visits, with the final follow-up deadline set as May 31, 2024. Mode of death was determined from medical records, hospital death reports, and death certificates. If necessary, further medical information about events that occurred at the time of death was obtained from interviews with the patient's primary care provider, family members, or witnesses. The mode of death was defined as the first clinically relevant event preceding the death. Cardiac deaths, including HF death (worsening HF), sudden cardiac death, cardiogenic shock, and fatal arrhythmias, were classified as positive cases and included in the cardiac death group. Survivors and patients who died from non-cardiac causes, such as pulmonary infection, sepsis, or renal failure, were collectively categorized as the non-cardiac death group.

Feature selection, model training and performance evaluation

This study employed five machine learning methods for model training: Logistic Regression (LR), Classification and Regression Tree (CART), Random Forest (RF), Support Vector Machine (SVM), and eXtreme Gradient Boosting (XGBoost). Before the feature extraction of machine learning, univariate analyses were conducted on all clinical variables to identify those with statistically significant differences between the cardiac death and non-cardiac groups ($p < 0.05$). Subsequently, LASSO regression was used for feature selection in the LR model, while recursive feature elimination was applied for the RF and SVM models. The XGBoost and CART models were trained using all variables. Model performance was evaluated using receiver operating characteristic (ROC) curves, calibration curves, decision curve analysis (DCA), radar charts (including area under the curve [AUC], accuracy, precision, recall, specificity, and F1-score), and confusion matrices. Feature importance ranking plots and the nomogram were utilized to visualize the model.

After selecting the optimal model, the predictive model was compared against previously established classic staging systems, including the Mayo Clinic 2004 Staging System, Mayo Clinic 2012 Staging System, and European Modification 2015 of Mayo Staging System, to evaluate the clinical value of the newly developed model. Given that these legacy staging systems express outcomes as median survival times (MST), we assumed patients' survival time followed an exponential distribution (constant hazard rate) under non-intervention conditions. The survival probabilities were derived using the conversion formula:

$$S(t) = 2^{-t/MST}$$

where t represents target time and MST denotes median survival time. This transformation enabled direct comparison with survival probabilities generated by our model. The comparative results were visualized through ROC curve analysis and multidimensional radar charts.

Statistical analysis

Statistical analysis and data processing were conducted using R software. Measurement data were tested for normality and homogeneity of variance. Variables following a normal distribution were presented as mean ± standard deviation and analyzed using the independent samples t-test. Non-normally distributed variables were presented as median (interquartile range [IQR]) and analyzed using non-parametric tests. Enumeration data were expressed as rates and analyzed using the χ^2 test or Fisher's exact test. A p-value < 0.05 was considered statistically significant.

Study variable definitions

This study incorporated a wide range of clinical data variables. Based on general consensus and informed by previous literature, clear and consistent definitions were established for these variables. Comprehensive definitions for all variables are provided in Supplementary Material 1.

Results

Patient characteristics

A total of 230 patients were ultimately included in the study after excluding 5 who did not meet the eligibility criteria (Fig. 1). In the training cohort (124 patients), 49 (39.5%) died due to cardiac causes, 10 (8.0%) died from

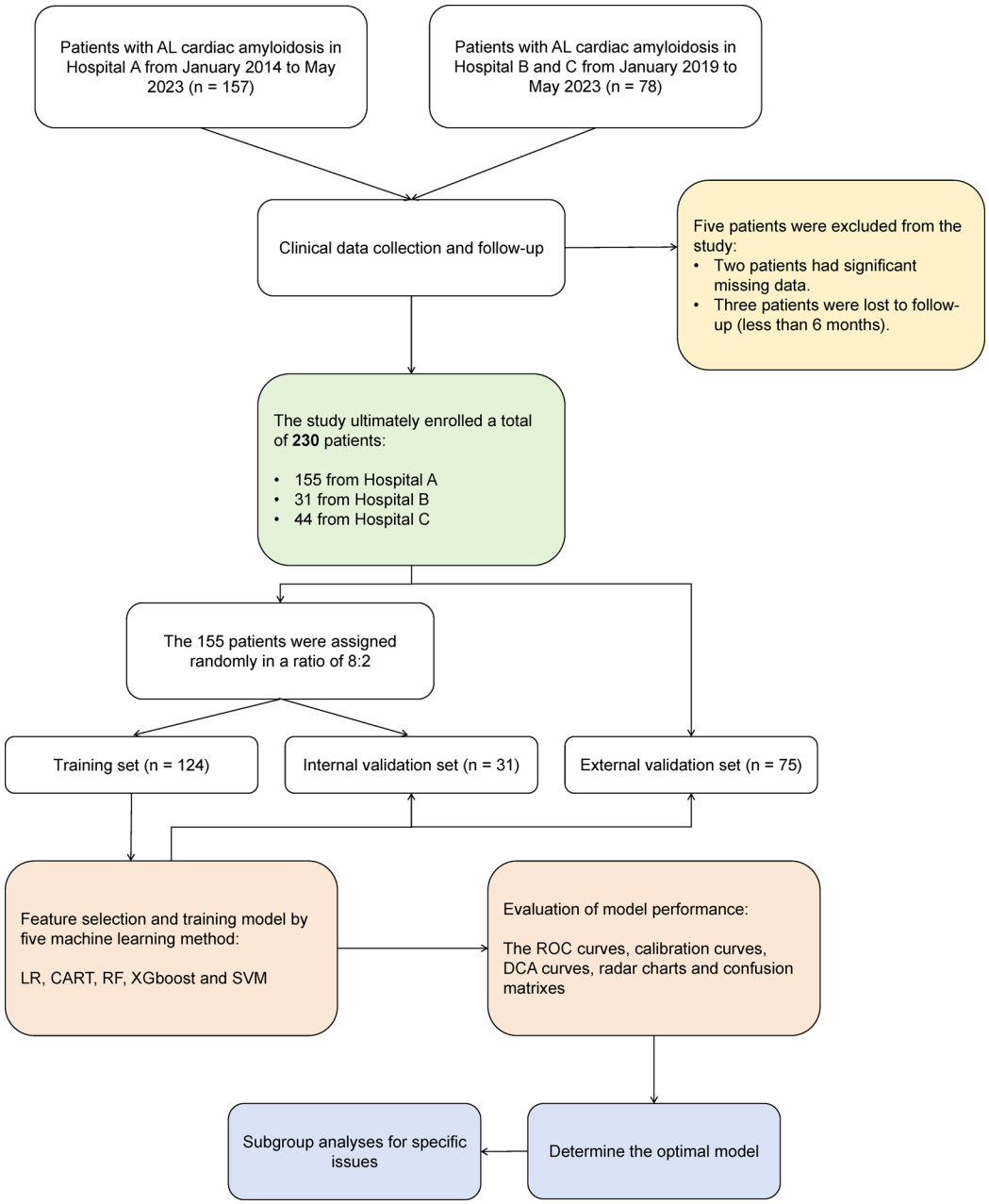

Fig. 1 Study flowchart

other causes, and 65 (52.4%) remained alive. Detailed baseline characteristics of this series are summarized in Table 1.

Model development

A total of 123 clinical features were collected as variables, and all underwent univariate analysis in the training set, with 66 variables showing statistically significant differences. Similar or collinear variables were eliminated, resulting in a total of 54 variables being included in the subsequent analysis. The comparison of feature differences between the training set and the internal validation set was not statistically significant, suggesting that the random grouping was appropriate (Supplementary Material 2). For the LR model, LASSO regression was employed for optimal feature selection (Fig. 2a and b), which resulted in the incorporation of 12 final features. Recursive feature elimination determined that the RF and SVM models required 53 and 26 optimal features, respectively, with the details provided in Fig. 2c and d.

Model verification and performance evaluation

Discrimination

The ROC curves of the five models in the three datasets are illustrated in Fig. 3a, b and c. The AUC for all five models in the training set exceeded 0.88, indicating excellent model fit. However, the RF and XGBoost models exhibited potential overfitting issues due to their excessively high AUCs. Notably, in external validation, all models demonstrated strong discriminative ability, with AUCs ranging from 0.817 to 0.877. DeLong's test was employed to compare the AUCs among these models, revealing no significant statistical differences (Supplementary Material 3).

Calibration

The five models demonstrated excellent calibration capability in the training set, as evidenced by their low Brier scores (BS) of less than 0.25. Among them, the RF, SVM, and XGBoost models achieved notably low BS values of 0.021, 0.048, and 0.002, respectively (Fig. 3d). Notably, the LR and RF models showed the best calibration performance, consistently displaying the lowest BS values in both the internal and external validation sets (Fig. 3e and f).

Decision curve analysis

The DCA results (Fig. 3g–i) show that all five models provide a net benefit across the entire threshold range of cardiac death probability in the training set. In internal validation, the LR model outperforms others by exhibiting net benefits throughout the entire threshold probability range, while the remaining models cover approximately 70%. In external validation, the RF model demonstrates net benefits over 86% of the threshold probabilities, with stable variation, signifying robust generalization ability. The LR model displays a clinical net benefit over 72% of the threshold probability spectrum (ranking third), yet it surpasses the RF model's net benefit markedly within the 0-70% cardiac death probability interval. A limitation of the LR model is its overly optimistic predictions regarding freedom from cardiac death for patients when their cardiac death risk is situated within the 73-98% threshold probability band. Nevertheless, the LR model demonstrates relatively stable and consistent DCA results across the three datasets. The ranges of threshold probabilities corresponding to net benefits, as derived from the DCA of the five models under external validation, are summarized in Supplementary Material 4.

Radar chart and confusion matrix

The Radar Chart (Fig. 3j–l) visualizes the comprehensive performance of the models, with all detailed data presented in Supplementary Material 5. In the training set, the RF and XGBoost models nearly attain a perfect score, standing out as the highest-fitting models. The internal validation highlights the LR model as significantly outperforming other models across all performance indicators. External validation suggests largely comparable performances among the five models, with the LR, RF, and SVM models performing slightly better.

The confusion matrix for the LR model in internal validation (the best-performing model) and the confusion matrices for all models in external validation are presented in Fig. 4. Notably, the LR model has a remarkably high true positive rate of 97%. Both the RF and SVM models share the highest true negative rate of 80%.

Visualization and nomogram

The RF model identified left ventricular ejection fraction (LVEF) as the strongest predictor of cardiac mortality, followed by NT-proBNP, BNP, and New York Heart Association (NYHA) functional class (Fig. 2e). Structural cardiac parameters including LV end-systolic diameter, early/late peak diastolic mitral inflow velocity (E/A) ratio, and left atrial dimensions, along with cTnI levels and lowest recorded mean arterial pressure (MAP) collectively contributed to risk stratification.

The nomogram, a visual presentation of the LR model, integrated 12 independent predictors, with impaired cardiac function (reduced LVEF, wall motion abnormalities, elevated E/A ratio), biomarker elevations (NT-proBNP and β2-microglobulin (β2M)), clinical decompensation signs (NYHA III-IV, syncope/presyncope, pericardial effusion, decreased MAP), and electrical instability (concomitant VA, left axis deviation (LAD) on ECG) contributing predominantly. Notably, the absence of autologous

Table 1 Patient characteristics of the training set

Variables	Total ($n=124$)	Cardiac death ($n=49$)	Non-cardiac death ($n=75$)	p value
Demographic and Clinical Characteristics				
Age at diagnosis (years), Mean ± SD	59.87 ± 9.24	59.82 ± 9.92	59.91 ± 8.84	0.958
Age at symptom onset (years), Mean ± SD	59.08 ± 9.30	59.12 ± 9.65	59.05 ± 9.14	0.968
Male sex, n (%)	80 (64.52)	32 (65.31)	48 (64.00)	0.882
Height (cm), Median (IQR)	167.00 (160.00, 170.25)	165.00 (160.00, 171.00)	167.00 (160.00, 170.00)	0.632
Weight (kg), Median (IQR)	64.00 (58.00, 71.25)	64.00 (57.50, 71.00)	64.00 (58.00, 72.00)	0.814
Body mass index (kg/m^2), Median (IQR)	23.19 (21.68, 25.38)	23.02 (21.88, 24.97)	23.34 (21.47, 26.08)	1.000
Body surface area (m^2), Median (IQR)	1.69 (1.56, 1.81)	1.67 (1.56, 1.82)	1.69 (1.59, 1.80)	0.671
Mayo Clinic 2004 Staging System				< 0.001
Stage 1, n (%)	15 (12.1)	0 (0.0)	15 (20.0)	
Stage 2, n (%)	60 (48.4)	20 (40.8)	40 (53.3)	
Stage 3, n (%)	49 (39.5)	29 (59.2)	20 (26.7)	
Mayo Clinic 2012 Staging System				< 0.001
Stage 1, n (%)	33 (26.6)	3 (6.1)	30 (40.0)	
Stage 2, n (%)	34 (27.4)	14 (28.6)	20 (26.7)	
Stage 3, n (%)	49 (39.5)	27 (55.1)	22 (29.3)	
Stage 4, n (%)	8 (6.5)	5 (10.2)	3 (4.0)	
European Modification 2015 of Mayo Staging System				< 0.001
Stage 1, n (%)	15 (12.1)	0 (0.0)	15 (20.0)	
Stage 2, n (%)	60 (48.4)	20 (40.8)	40 (53.3)	
Stage 3a, n (%)	32 (25.8)	19 (38.8)	13 (17.3)	
Stage 3b, n (%)	17 (13.7)	10 (20.4)	7 (9.3)	
NYHA functional class, Median (IQR)	2.00 (1.00, 2.25)	2.00 (2.00, 3.00)	1.00 (1.00, 2.00)	< 0.001
Time from symptom onset to diagnosis (months), Median (IQR)	6.00 (2.00, 12.00)	6.00 (2.00, 12.00)	6.00 (2.50, 12.00)	0.841
Cardiac manifestations as initial presentation, n (%)	34 (27.42)	23 (46.94)	11 (14.67)	< 0.001
History of hypotension, n (%)	21 (16.94)	13 (26.53)	8 (10.67)	0.021
Syncope/presyncope episodes, n (%)	10 (8.06)	9 (18.37)	1 (1.33)	0.002
Initial admission MAP (mmHg), Mean ± SD	90.22 ± 12.12	87.91 ± 14.05	91.72 ± 10.51	0.108
Initial admission SBP (mmHg), Median (IQR)	123.00 (110.00, 132.50)	120.00 (99.00, 135.00)	125.00 (114.00, 131.50)	0.181
Initial admission DBP (mmHg), Median (IQR)	75.00 (68.00, 80.00)	70.00 (66.00, 80.00)	77.00 (70.00, 80.00)	0.069
Lowest recorded MAP (mmHg), Median (IQR)	85.67 (72.92, 92.33)	76.67 (68.33, 86.67)	87.00 (82.00, 93.33)	0.001
Lowest recorded SBP (mmHg), Median (IQR)	118.00 (97.00, 125.25)	100.00 (90.00, 120.00)	120.00 (110.00, 126.00)	0.005
Lowest recorded MAP (mmHg), Median (IQR)	70.00 (60.00, 76.00)	62.00 (56.00, 70.00)	71.00 (67.00, 78.00)	0.001
Hypertension, n (%)	52 (41.94)	23 (46.94)	29 (38.67)	0.361
Coronary artery disease, n (%)	23 (18.55)	11 (22.45)	12 (16.00)	0.366
Myocardial infarction history, n (%)	6 (4.84)	3 (6.12)	3 (4.00)	0.912
Chronic kidney disease, n (%)	54 (43.55)	27 (55.10)	27 (36.00)	0.036
Hepatic dysfunction, n (%)	21 (16.94)	13 (26.53)	8 (10.67)	0.021
Hyperlipidemia, n (%)	45 (36.29)	16 (32.65)	29 (38.67)	0.496
Multiple myeloma, n (%)	81 (65.32)	33 (67.35)	48 (64.00)	0.702
Chemotherapy, n (%)	98 (79.03)	34 (69.39)	64 (85.33)	0.033
Autologous stem cell transplantation, n (%)	14 (11.29)	1 (2.04)	13 (17.33)	0.009
Organs with amyloid deposition				
Renal involvement, n (%)	102 (82.26)	43 (87.76)	59 (78.67)	0.195
Soft tissue involvement, n (%)	30 (24.19)	10 (20.41)	20 (26.67)	0.426
Neurological involvement, n (%)	38 (30.65)	10 (20.41)	28 (37.33)	0.046
Gastrointestinal involvement, n (%)	6 (4.84)	4 (8.16)	2 (2.67)	0.334
Pulmonary involvement, n (%)	3 (2.42)	1 (2.04)	2 (2.67)	1.000
Hepatic involvement, n (%)	25 (20.16)	16 (32.65)	9 (12.00)	0.005
Total number of involved organs, Median (IQR)	2.00 (2.00, 3.00)	3.00 (2.00, 3.00)	2.00 (2.00, 3.00)	0.131
ECG features				
Heart rate (bpm), Mean ± SD	85.38 ± 14.05	84.82 ± 11.92	85.75 ± 15.35	0.720

Table 1 (continued)

Variables	Total ($n=124$)	Cardiac death ($n=49$)	Non-cardiac death ($n=75$)	p value
PR interval (ms), Mean ± SD	159.79 ± 26.32	165.59 ± 25.89	156.00 ± 26.08	0.047
P-wave duration (ms), Median (IQR)	90.00 (84.00, 96.00)	90.00 (86.00, 96.00)	90.00 (82.00, 98.00)	0.840
QRS duration (ms), Median (IQR)	88.50 (82.00, 94.00)	92.00 (84.00, 98.00)	86.00 (82.00, 92.00)	0.003
Corrected QT interval (ms), Median (IQR)	428.00 (404.00, 450.50)	435.00 (414.00, 471.00)	425.00 (403.00, 443.50)	0.079
QRS axis (degrees), Median (IQR)	30.50 (-39.00, 58.00)	4.00 (-54.00, 50.00)	35.00 (-5.00, 59.00)	0.094
R-wave amplitude in lead V5 (mV), Median (IQR)	0.96 (0.58, 1.38)	0.80 (0.34, 1.08)	1.12 (0.68, 1.52)	0.006
S-wave amplitude in lead V1 (mV), Median (IQR)	0.65 (0.45, 0.93)	0.65 (0.49, 0.92)	0.63 (0.41, 0.94)	0.838
Sokolow-Lyon index (mV), Median (IQR)	1.46 (0.79, 2.52)	1.23 (0.55, 2.48)	1.56 (1.07, 2.54)	0.073
R-wave in V5/S-wave in V1 ratio, Median (IQR)	1.63 (1.13, 2.21)	1.45 (0.98, 1.92)	1.74 (1.21, 2.35)	0.024
Minimum limb lead voltage (mV), Median (IQR)	0.20 (0.15, 0.30)	0.20 (0.10, 0.30)	0.25 (0.20, 0.30)	0.127
Maximum limb lead voltage (mV), Median (IQR)	0.65 (0.45, 0.85)	0.55 (0.45, 0.80)	0.70 (0.50, 0.88)	0.092
Mean limb lead voltage (mV), Median (IQR)	0.45 (0.33, 0.59)	0.42 (0.29, 0.56)	0.47 (0.36, 0.60)	0.149
QRS axis deviation (degrees), Median (IQR)	35.00 (14.00, 84.00)	68.00 (26.00, 99.00)	32.00 (11.50, 61.50)	0.009
Low Sokolow-Lyon index (< 1.5), n (%)	56 (45.16)	28 (57.14)	28 (37.33)	0.030
Low limb lead voltage, n (%)	56 (45.16)	30 (61.22)	26 (34.67)	0.004
Low precordial lead voltage, n (%)	29 (23.39)	17 (34.69)	12 (16.00)	0.016
Pseudo-infarct pattern, n (%)	39 (31.45)	21 (42.86)	18 (24.00)	0.027
Impaired R-wave progression, n (%)	39 (31.45)	21 (42.86)	18 (24.00)	0.027
Arrhythmias, n (%)	31 (25.00)	22 (44.90)	9 (12.00)	< 0.001
Bradycardia and conduction abnormalities, n (%)	33 (26.61)	23 (46.94)	10 (13.33)	< 0.001
T-wave abnormality, n (%)	51 (41.13)	28 (57.14)	23 (30.67)	0.003
ST-segment abnormalities, n (%)	19 (15.32)	8 (16.33)	11 (14.67)	0.802
Fragmented QRS complexes, n (%)	12 (9.68)	7 (14.29)	5 (6.67)	0.275
Atrial arrhythmias, n (%)	20 (16.13)	11 (22.45)	9 (12.00)	0.122
Ventricular arrhythmias, n (%)	16 (12.90)	14 (28.57)	2 (2.67)	< 0.001
Left axis deviation, n (%)	44 (35.48)	23 (46.94)	21 (28.00)	0.031
Echocardiographic features				
LV end-diastolic diameter (mm), Mean ± SD	45.79 ± 5.36	45.71 ± 6.22	45.85 ± 4.75	0.901
LV end-systolic diameter (mm), Median (IQR)	29.00 (26.75, 32.25)	31.00 (29.00, 36.00)	28.00 (26.00, 30.50)	< 0.001
LVEF (%), Median (IQR)	64.00 (56.75, 69.00)	56.00 (47.00, 65.00)	66.00 (62.00, 71.00)	< 0.001
Left atrial anteroposterior diameter (mm), Mean ± SD	38.86 ± 5.51	41.22 ± 4.57	37.32 ± 5.56	< 0.001
Left atrial transverse diameter (mm), Mean ± SD	40.74 ± 5.80	42.60 ± 4.51	39.53 ± 6.24	0.002
Left atrial longitudinal diameter (mm), Median (IQR)	53.00 (49.00, 56.00)	54.00 (53.00, 57.00)	50.00 (46.00, 53.00)	< 0.001
Left atrial diameter index, Mean ± SD	23.00 ± 3.58	24.59 ± 3.60	21.96 ± 3.18	< 0.001
Right atrial transverse diameter (mm), Median (IQR)	36.00 (33.00, 39.00)	38.00 (36.00, 42.00)	35.00 (32.50, 37.00)	< 0.001
Right atrial anteroposterior diameter (mm), Median (IQR)	47.00 (44.00, 51.00)	50.00 (47.00, 54.00)	46.00 (42.85, 50.00)	< 0.001
Right ventricular diameter (mm), Median (IQR)	33.00 (30.00, 37.00)	35.00 (32.00, 38.00)	31.00 (29.00, 36.00)	0.002
LV mass (g), Median (IQR)	201.33 (164.45, 257.14)	216.55 (188.02, 262.62)	189.19 (147.83, 243.88)	0.007
LV mass index (g/m^2), Median (IQR)	118.96 (95.40, 150.37)	130.87 (108.14, 158.08)	106.72 (87.73, 143.43)	0.005
Interventricular septal thickness (mm), Median (IQR)	12.30 (10.00, 14.00)	13.00 (11.30, 15.00)	12.00 (10.00, 13.65)	0.008
LV posterior wall thickness (mm), Median (IQR)	11.40 (10.00, 13.00)	12.00 (11.00, 15.00)	11.00 (10.00, 12.40)	0.002
LV relative wall thickness, Median (IQR)	0.49 (0.42, 0.58)	0.54 (0.43, 0.64)	0.48 (0.40, 0.56)	0.011
LV hypertrophy, n (%)	65 (52.42)	34 (69.39)	31 (41.33)	0.002
Aortic diameter (mm), Median (IQR)	31.00 (29.00, 33.00)	31.00 (29.00, 33.00)	31.00 (29.50, 33.00)	0.937
Ascending aorta diameter (mm), Mean ± SD	33.45 ± 3.81	33.53 ± 3.86	33.40 ± 3.79	0.856
Pulmonary artery diameter (mm), Median (IQR)	25.00 (24.00, 27.00)	26.00 (24.00, 28.00)	25.00 (23.00, 26.50)	0.006
E-wave (m/s), Median (IQR)	89.50 (73.00, 105.25)	97.00 (84.00, 115.00)	85.00 (66.50, 95.50)	< 0.001
A-wave (m/s), Mean ± SD	81.94 ± 26.86	74.80 ± 29.10	86.60 ± 24.37	0.016
E/A ratio, Median (IQR)	1.15 (0.76, 1.46)	1.29 (1.14, 1.92)	0.86 (0.73, 1.21)	< 0.001
Pericardial effusion (grade), Median (IQR)	0.00 (0.00, 2.00)	1.00 (0.00, 2.00)	0.00 (0.00, 1.00)	< 0.001
Valvular regurgitation (grade), Median (IQR)	2.00 (1.00, 2.00)	2.00 (2.00, 3.00)	2.00 (1.00, 2.00)	< 0.001
Valvular thickening, n (%)	17 (13.71)	6 (12.24)	11 (14.67)	0.701

Table 1 (continued)

Variables	Total ($n=124$)	Cardiac death ($n=49$)	Non-cardiac death ($n=75$)	p value
Wall motion abnormality, n (%)	25 (20.16)	19 (38.78)	6 (8.00)	< 0.001
LV systolic dysfunction, n (%)	25 (20.16)	21 (42.86)	4 (5.33)	< 0.001
LV diastolic dysfunction, n (%)	94 (75.81)	39 (79.59)	55 (73.33)	0.426
Right ventricular systolic dysfunction, n (%)	12 (9.68)	8 (16.33)	4 (5.33)	0.087
Pulmonary arterial hypertension, n (%)	34 (27.42)	21 (42.86)	13 (17.33)	0.002
Combined ECG and echocardiographic parameters				
Limb leads QRS score to LV wall thickness ratio, Median (IQR)	0.23 (0.16, 0.33)	0.20 (0.12, 0.30)	0.24 (0.17, 0.34)	0.011
Sokolow-Lyon index / LV posterior wall thickness, Median (IQR)	1.50 (0.92, 2.05)	1.23 (0.72, 1.68)	1.73 (1.00, 2.22)	0.004
Sokolow-Lyon index / LV relative wall thickness, Median (IQR)	32.13 (20.68, 49.79)	28.75 (15.05, 40.00)	39.75 (23.04, 53.41)	0.010
Sokolow-Lyon index / LV mass, Median (IQR)	0.08 (0.05, 0.12)	0.07 (0.04, 0.10)	0.11 (0.06, 0.13)	0.001
Voltage-to-mass ratio, Median (IQR)	0.14 (0.09, 0.21)	0.11 (0.07, 0.15)	0.17 (0.10, 0.23)	0.001
Laboratory examination				
Cardiac troponin I (ng/mL), Median (IQR)	0.06 (0.02, 0.21)	0.12 (0.05, 0.25)	0.03 (0.01, 0.11)	0.002
BNP (pg/mL), Median (IQR)	403.92 (133.52, 1339.66)	1202.24 (407.20, 2986.00)	202.00 (72.98, 724.00)	< 0.001
NT-proBNP (pg/mL), Median (IQR)	3149.00 (849.83, 7746.75)	6204.00 (3846.00, 13306.25)	1537.50 (456.10, 4525.00)	< 0.001
Serum albumin (g/L), Median (IQR)	32.90 (26.65, 36.52)	33.60 (29.40, 36.50)	32.30 (24.65, 36.60)	0.297
Serum globulin (g/L), Median (IQR)	25.50 (20.17, 32.85)	27.50 (21.20, 32.40)	24.00 (19.70, 32.90)	0.252
Serum total protein (g/L), Median (IQR)	59.80 (50.43, 69.60)	62.30 (55.30, 68.80)	59.00 (48.55, 70.10)	0.342
Albumin-to-globulin ratio, Mean ± SD	1.24 ± 0.54	1.22 ± 0.50	1.26 ± 0.57	0.690
Serum creatinine (μmol/L), Median (IQR)	85.00 (65.40, 150.53)	96.50 (71.90, 216.80)	81.60 (63.90, 123.65)	0.070
Creatinine clearance (mL/min), Median (IQR)	71.10 (39.38, 93.36)	68.92 (26.50, 79.18)	74.42 (50.85, 96.12)	0.068
β2-Microglobulin (mg/L), Median (IQR)	4.83 (2.94, 7.35)	5.30 (3.10, 9.86)	4.14 (2.90, 6.29)	0.037
ALT (U/L), Median (IQR)	18.00 (13.00, 26.00)	18.00 (12.00, 29.00)	18.00 (13.50, 23.50)	0.446
AST (U/L), Median (IQR)	22.50 (17.00, 29.00)	24.00 (19.00, 36.00)	22.00 (16.00, 25.00)	0.024
AST-to-ALT ratio, Median (IQR)	1.27 (0.95, 1.55)	1.33 (1.00, 1.57)	1.21 (0.95, 1.52)	0.421
Serum calcium (mmol/L), Median (IQR)	2.16 (2.01, 2.29)	2.16 (2.01, 2.28)	2.17 (2.01, 2.31)	0.988
Hemoglobin (g/L), Median (IQR)	107.50 (83.50, 126.50)	106.00 (82.00, 118.00)	113.00 (84.50, 132.00)	0.147
White blood cell count ($\times 10^9$/L), Median (IQR)	6.01 (5.00, 7.62)	5.71 (4.98, 7.70)	6.09 (5.08, 7.50)	0.609
Platelet count ($\times 10^9$/L), Median (IQR)	198.50 (138.00, 272.00)	168.00 (117.00, 236.00)	213.00 (164.00, 283.50)	0.014
Immunoglobulin G (mg/dL), Median (IQR)	666.50 (414.25, 1072.50)	769.00 (451.00, 1320.00)	643.00 (378.50, 889.00)	0.149
Immunoglobulin A (mg/dL), Median (IQR)	62.90 (31.15, 132.25)	53.30 (31.00, 93.40)	68.40 (32.55, 202.50)	0.138
Immunoglobulin M (mg/dL), Median (IQR)	31.65 (20.12, 48.82)	31.80 (19.20, 45.00)	31.50 (22.25, 50.85)	0.590
Immunoglobulin E (IU/mL), Median (IQR)	18.50 (17.70, 40.10)	18.50 (17.70, 42.80)	19.40 (17.70, 39.00)	0.739
Serum free light chain-λ (mg/dL), Median (IQR)	318.50 (195.50, 588.25)	413.00 (240.00, 715.00)	269.00 (182.00, 440.00)	0.002
Serum free light chain-κ (mg/dL), Median (IQR)	450.00 (295.25, 617.50)	402.00 (266.00, 526.00)	492.00 (322.00, 653.00)	0.022
Urine free light chain-λ (mg/dL), Median (IQR)	5.44 (5.00, 27.63)	16.50 (5.00, 48.40)	5.00 (5.00, 14.50)	0.005
Urine free light chain-κ (mg/dL), Median (IQR)	3.98 (1.85, 16.83)	4.20 (1.85, 16.90)	3.51 (1.85, 15.75)	0.985
Difference of free light chains (mg/dL), Median (IQR)	248.50 (102.50, 536.75)	244.00 (64.00, 542.00)	249.00 (116.00, 504.00)	0.354
Free light chain ratio, Median (IQR)	1.92 (1.34, 3.13)	1.72 (1.17, 3.79)	2.01 (1.39, 3.07)	0.200

t: t-test; Z: Mann-Whitney test; χ^2: Chi-square test; SD: Standard deviation; IQR: Interquartile range

Creatinine clearance is calculated by the Cockcroft-Gault formula

NYHA: New York Heart Association; MAP: mean arterial pressure; SBP: systolic blood pressure; DBP: diastolic blood pressure; LVEF: left ventricular ejection fraction; E-wave: Early diastolic mitral inflow velocity; A-wave: Late diastolic mitral inflow velocity; ALT: alanine aminotransferase; AST: aspartate aminotransferase

stem cell transplantation (ASCT) also emerged as one of the prognostic determinants. Risk stratification thresholds emerged with nomogram scores: 31 points conferred 1% mortality risk versus 99% at 216 points (Fig. 5).

After comparing from different perspectives, the LR and RF models outperformed other models in terms of performance, with both demonstrating considerable and comparable predictive capabilities. Considering practical clinical application, the LR model's nomogram offers greater applicability and interpretability. Therefore, the LR model was selected as the final prediction model.

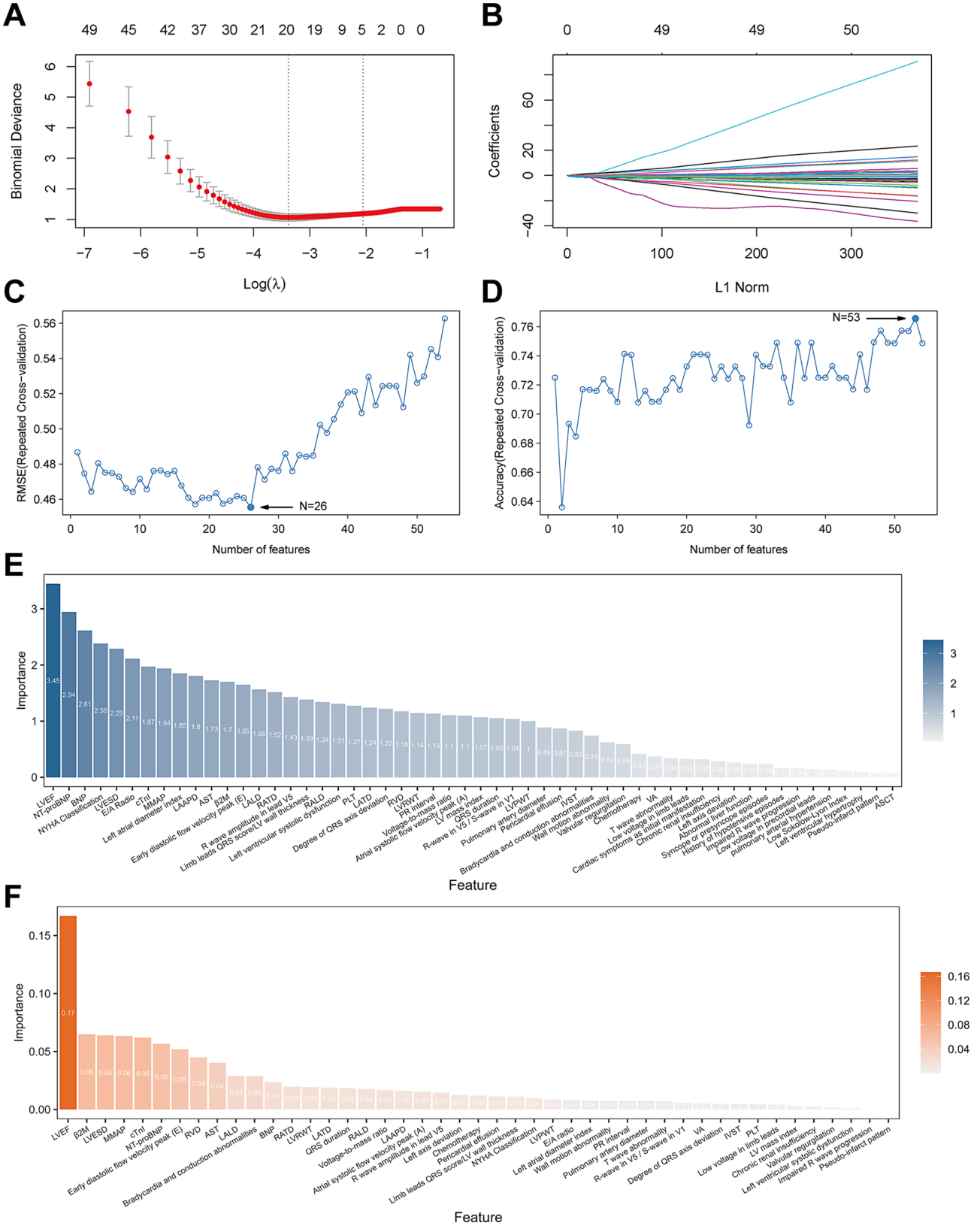

Fig. 2 (See legend on next page.)

(See figure on previous page.)

Fig. 2 Methodology and outcomes of the feature selection process for the machine learning models. (**a**) Five-fold cross-validation curve of LASSO Regression, indicating an optimal number of features at 19, subsequently reduced to 12 to prevent overfitting. (**b**) Coefficient path for LASSO Regression for all 54 features. (**c**) Optimal feature selection results for the SVM model using recursive feature elimination (RFE), achieving the lowest root mean square error with 26 features. (**d**) Optimal feature selection for the RF model using RFE, achieving peak accuracy with 53 features. (**e**) Ranking of feature importance in the RF model. (**f**) Ranking of feature importance in the XGBoost model

Comparison of performance with established staging systems

The survival probability conversion results for the established staging systems are presented in Supplementary Material 6. Our LR model achieved significantly higher AUC values than all existing systems in both Cohort 1 (training and internal validation set, $n = 155$) and Cohort 2 (external validation set, $n = 75$). These results are visualized in Fig. 6.

Additional analyses and noteworthy findings

As an additional analysis of this study, a descriptive statistical analysis was performed on the amalgamated cohort encompassing three distinct datasets. This analysis aimed to delineate the demographic and clinical profile of individuals with AL cardiac amyloidosis. Details are provided in Supplementary Material 7.

Furthermore, our prediction model analysis revealed several noteworthy findings:

Firstly, LAD was consistently associated with an increased risk of cardiac death in multiple models. In the amalgamated cohort, 27.4% had LAD, with 95.2% (60/63) showing a typical left anterior fascicular block pattern. There was a significant difference in LAD between patients with cardiac death and those without (40.0% vs. 18.5%, $p < 0.001$), see Supplementary Material 8. However, only a very small number of patients exhibited left posterior fascicular block (0.9%), right bundle branch block (5.7%), and left bundle branch block (0.9%). This finding has not been previously reported.

Secondly, β2M level was identified as an important predictor of cardiac death, unexpectedly surpassing other renal function indicators such as creatinine and creatinine clearance rate.

Thirdly, BNP vs. NT-proBNP: NT-proBNP demonstrated higher predictive value compared to BNP across all models, indicating its superiority in evaluating cardiac prognosis and the risk of cardiac death in AL amyloidosis patients.

Fourthly, in this study, 8 patients (3.5% of the total cohort, $n = 230$) ultimately underwent pacemaker (PM) or implantable cardioverter-defibrillator (ICD) implantation. Among the 230 patients, 23 (10.0%) met clinical indications for PM/ICD implantation, including 14 patients with pacemaker indications (10 cases of sick sinus syndrome and 4 cases of high-grade or third-degree atrioventricular block). Of these 23 patients, 8 received PM/ICD implantation with a survival rate of 50% (4/8), while the remaining 15 patients declined or deferred intervention and exhibited a survival rate of 20% (3/15). A chi-square test comparing the two groups yielded a p-value of 0.135. Although the observed survival difference suggests potential clinical benefit from PM/ICD implantation, the limited sample size precludes definitive statistical significance.

These findings provide novel insights into the prediction of cardiac outcomes in AL amyloidosis.

Discussion

Main findings

This study develops a novel prediction model and scoring system to forecast the risk of cardiac death in AL amyloidosis patients, with validated performance. Additionally, several previously unreported clinical features associated with cardiac prognosis, including LAD, E/A ratio, and β2M level, were discovered for the first time.

Comparison of the new cardiac prognostic model and conventional staging systems

The prognosis for patients with systemic AL amyloidosis remains challenging, with cardiac death being a critical factor [1, 17, 18]. HF and sudden death account for 55% of all deaths in AL amyloidosis patients, and represent 63.6% of all deaths in AL cardiac amyloidosis patients, with early cardiac deaths predominating over non-cardiac causes such as renal failure [19, 20]. In particular, the risk of early sudden cardiac death is challenging to detect initially [3, 20].

Previous research has developed staging systems to evaluate outcomes [8–10]. In 2024, a simple frailty score using age, Eastern Cooperative Oncology Group performance status, and NT-proBNP was developed [11]. Another study identified prognostic indicators including Creatine Kinase MB isoenzyme, estimated glomerular filtration rate (eGFR), interventricular septal thickness, LVEF, and alanine aminotransferase, aiming to predict the survival time based on multi-organ involvement [12]. However, these systems lack emphasis on the risk of cardiac death, particularly early sudden death. A recent study demonstrated that a combination of pericardial effusion, low QRS voltages, impaired global radial strain derived from cardiac magnetic resonance (CMR), and LV wall thickening can reflect the risk of death to a certain extent, but quantitative results of the predictive death risk were not provided [21].

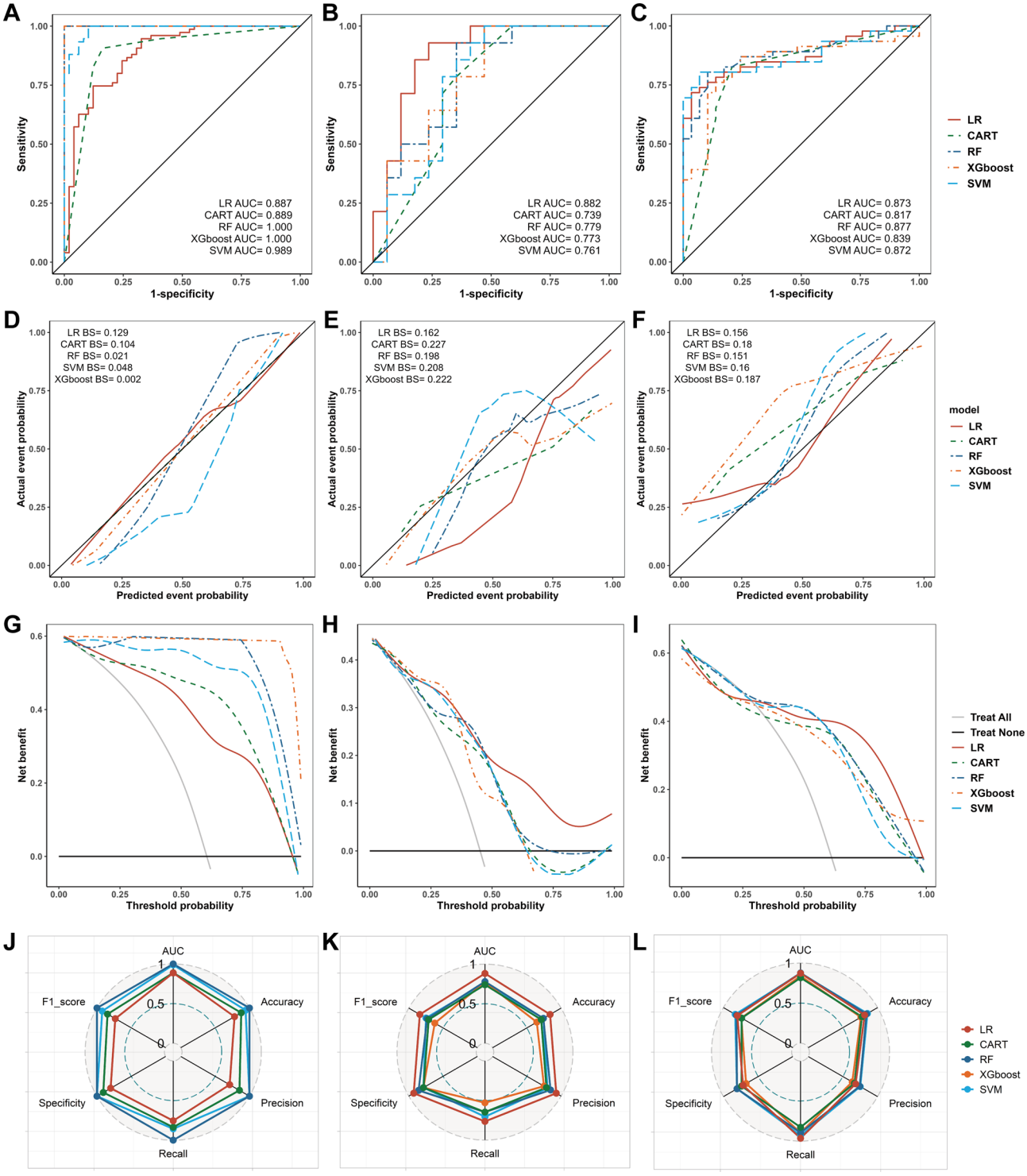

Fig. 3 Model performance evaluation across three datasets. **a**-**c**. ROC curves and AUCs for the five models. (**a**) Training set. (**b**) Internal validation set. (**c**) External validation set. **d**-**f**.Calibration curves and Brier scores for the five models. (**d**) Training set. (**e**) Internal validation set. (**f**) External validation set. **g**-**i**. DCA for the five models. (**g**) Training set. (**h**) Internal validation set. (i) External validation set. **j**-**l**. Radar charts for the five models. (**j**) Training set. **k.** Internal validation set. **l.** External validation set

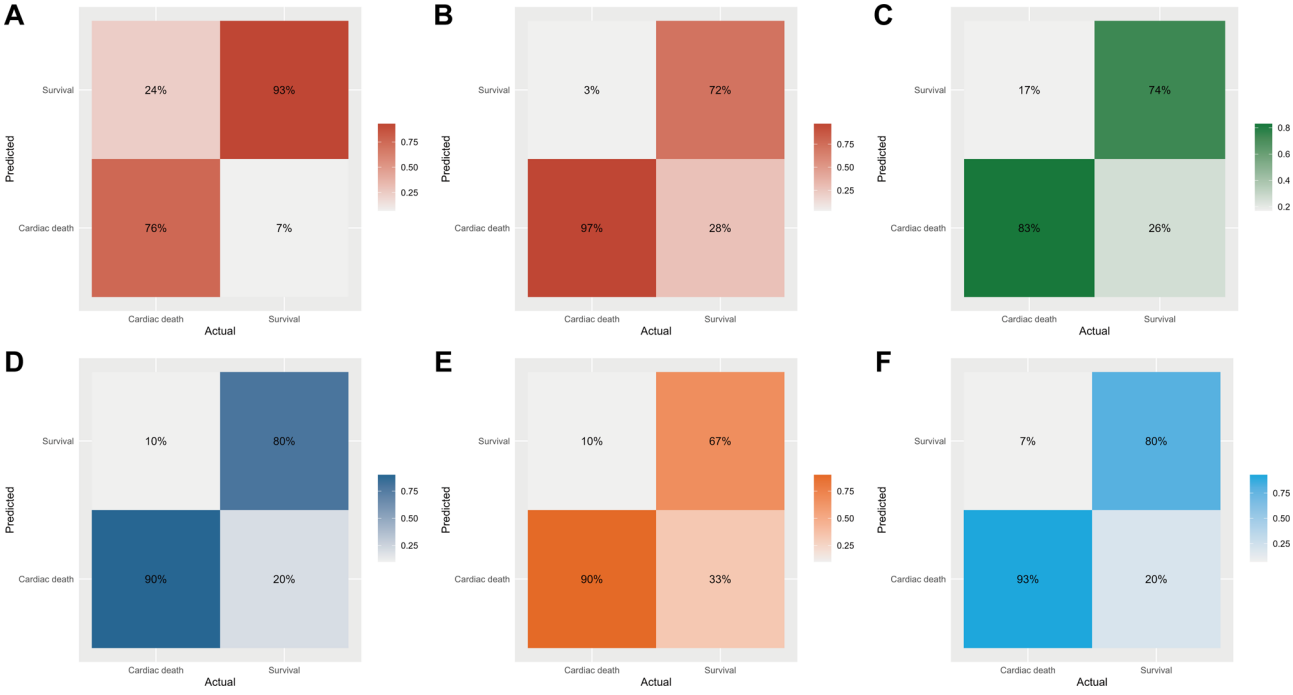

Fig. 4 Confusion matrix of five models. **a.** LR model in the internal validation, **b**-**f.** LR, CART, RF, XGBoost, and SVM models in the external validation, respectively

We acknowledge that, although several staging systems for AL amyloidosis in clinical practice hold significant importance, these systems still exhibit limitations.

Limitations of existing staging systems

The Mayo 2004 staging system, the most classical system for AL amyloidosis, classifies patients into three stages with median survival times of 26.4, 10.5, and 3.5 months, respectively [8]. However, a significant proportion of clinically diagnosed AL amyloidosis patients fall into Stage 2. While some Stage 2 patients experience early cardiac sudden death, others survive far beyond the predicted 10.5 months, highlighting the system's limited discriminative capacity in this "gray-zone" population. The Mayo 2012 system introduced the difference in free light chains (dFLC) as a prognostic factor [9]. Although we initially included dFLC and serum free light chain ratio as potential predictors in our machine learning model, these variables failed to demonstrate satisfactory predictive value for early cardiac death. In contrast, the variables ultimately selected in our model showed superior performance. The European 2015 modification of the Mayo 2004 system introduced a very-high-risk subgroup (Stage 3b) [22]. However, the 3-year survival rates for Stage 2 (55%) and Stage 3a (52%) patients remain clinically indistinct, underscoring its limited prognostic utility.

To validate our model's superiority, we quantitatively compared its predictive performance with the Mayo 2004, Mayo 2012, and European 2015 systems, and our model achieved significantly higher performance than all existing systems in both cohorts.

Impact of modern therapies

Recent advances in treatment regimens, including cyclophosphamide-bortezomib-dexamethasone (VCD) and particularly daratumumab-based therapies, have significantly prolonged survival in AL amyloidosis patients [23–28]. Consequently, the prognostic accuracy of historical staging systems may be compromised. Our study cohort (2014–2023, with validation from 2019 to 2023) incorporates patients managed under contemporary therapeutic paradigms, ensuring our model serves as a timely update and complement to classical systems.

Cardiac-Specific prognostication

Existing staging systems evaluate overall survival (all-cause mortality) rather than cardiac-specific outcomes. In contrast, our model was explicitly designed and trained to predict cardiac death, excluding non-cardiac causes (e.g., renal failure). This specificity enhances its utility for identifying high-risk patients requiring targeted cardiac monitoring and preventive interventions.

Clinical accessibility

While our model does not incorporate advanced imaging modalities like CMR or speckle-tracking echocardiography, it relies on readily available clinical and laboratory

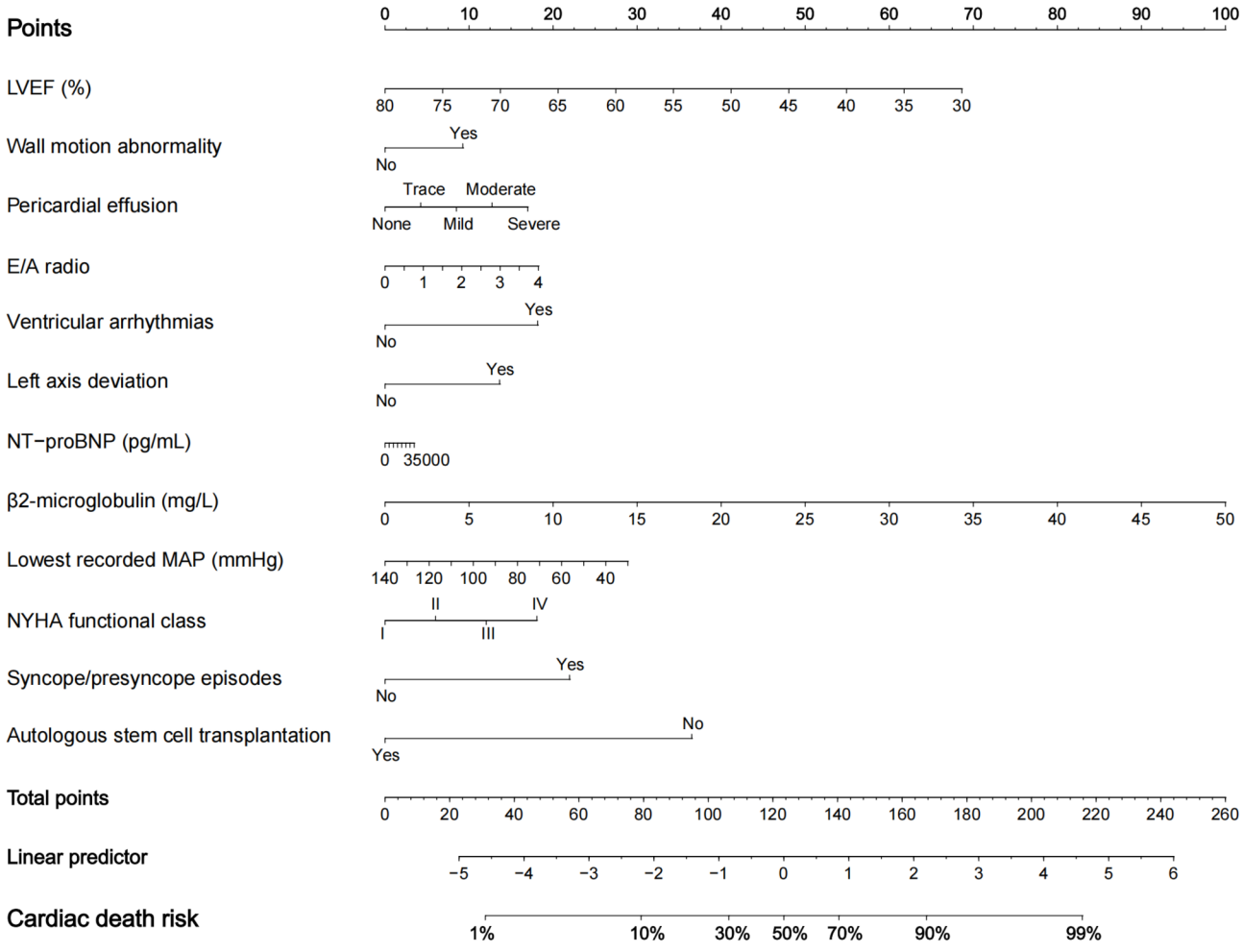

Fig. 5 Nomogram of the final prediction model (LR model)

parameters. This design ensures practical applicability in resource-limited settings.

Underlying mechanisms linking clinical features to cardiac outcomes

We found that LVEF is the most powerful predictor of cardiac prognosis. On one hand, despite AL cardiac amyloidosis primarily characterized by diastolic dysfunction and often presenting with HF with preserved ejection fraction in the early stages, progressive decline in left ventricular systolic function occurs as the disease progresses [17]. On the other hand, with ongoing amyloid infiltration and its toxic effects on the myocardium, HF exacerbation is often accompanied by conduction system abnormalities and can lead to VA or conduction blocks, increasing the risk of mortality [29].

Similarly, the presence of wall motion abnormalities is a useful predictive feature. These abnormalities not only reflect the severity of amyloid infiltration in the LV myocardium but also indicate the potential for acute myocardial injury and myocardial infarction due to amyloid infiltration of the coronary arteries and their surrounding tissues, even in the absence of atherosclerotic coronary artery disease [30, 31]. Localized wall motion abnormalities may signify the presence of amyloid-related coronary artery disease and suggest a risk for future myocardial infarction [32, 33].

The E/A ratio is a useful prognostic clinical feature, primarily used to assess mitral valve hemodynamics and LV diastolic function. It is typically elevated in moderate to severe LV diastolic dysfunction and severe mitral regurgitation (MR). In AL amyloidosis, severe LV diastolic dysfunction indicates widespread amyloid deposition and advanced disease, often signaling poor prognosis. Moderate to severe MR and tricuspid regurgitation have been previously shown to be associated with adverse outcomes in HF populations [34, 35]. Data on valvular disease in AL cardiac amyloidosis indicate that the most common valvular abnormalities are tricuspid regurgitation (52.8%) and MR (47.2%) [36]. In our study, these proportions appear to be higher. Recent studies demonstrate that patients with moderate to severe mitral and tricuspid

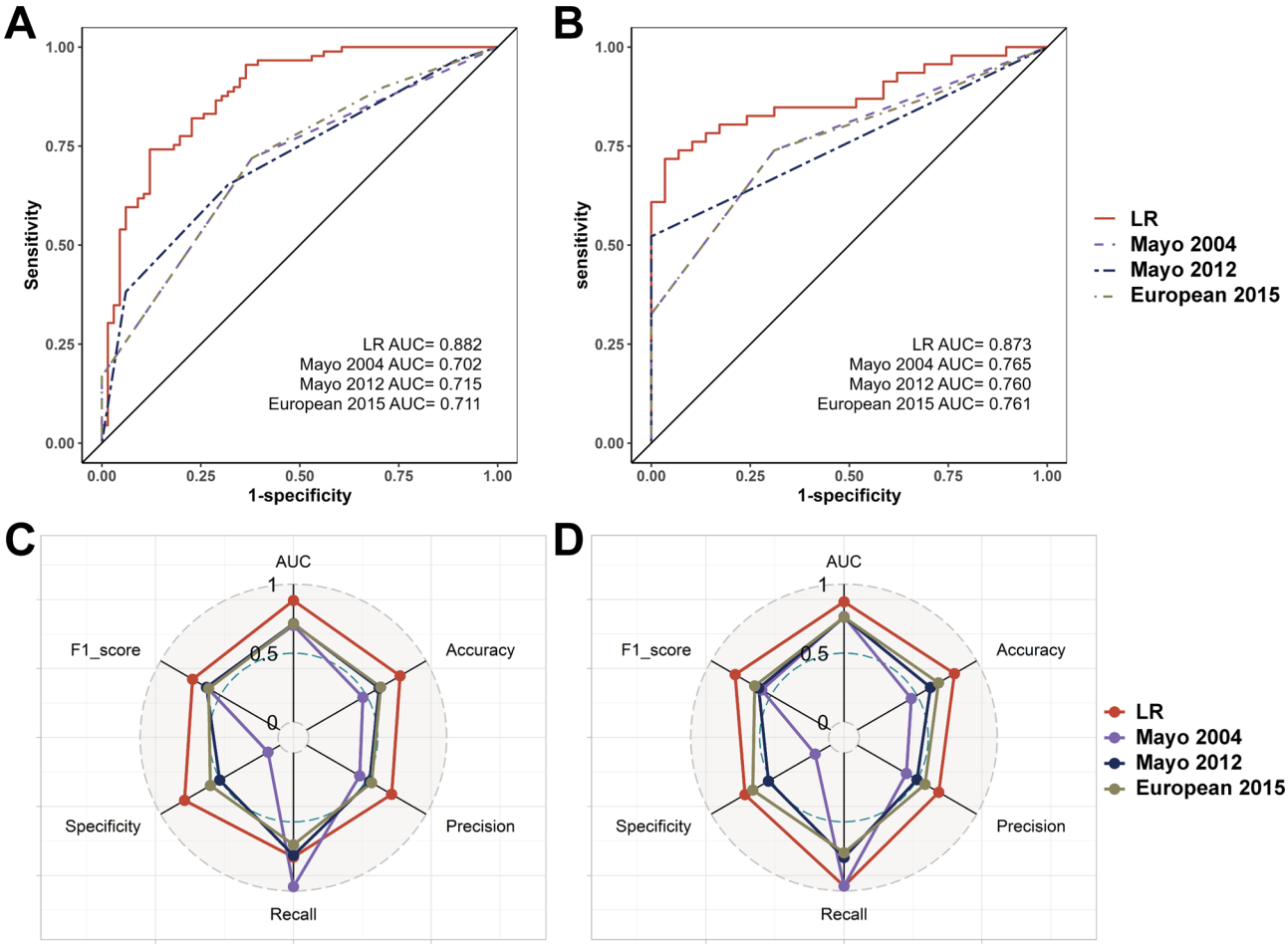

Fig. 6 Comparison of performance with established staging systems. (**a**) ROC curves for the training/internal validation set; (**b**) ROC curves for the external validation set; (**c**) Radar chart for the training/internal validation set; (**d**) Radar plot for the external validation set

regurgitation tend to have more severe symptoms, higher NT-proBNP and cardiac troponin levels, and are independently associated with increased risk of all-cause mortality or worsening HF [37]. Atrial functional MR is considered the most common cause of MR in this population. However, whether treating MR in patients with cardiac amyloidosis improves the clinical course of the disease and attenuates the progression of four-chamber remodeling remains unexplored and warrants further investigation.

Notably, our findings indicate that β2M emerges as a robust predictor of cardiac outcomes. This may be due to its reflection of underlying HF and multi-organ dysfunction. On one hand, its elevation is common in renal dysfunction and hematological malignancies, such as MM, where it serves as an independent prognostic marker for survival and can predict the likelihood of renal function response, recovery, and dialysis dependence [38, 39]. The β2M decline index, based on pre- and post-treatment changes, predicts MM treatment efficacy and survival [40]. On the other hand, increasing clinical evidence shows that β2M levels correlate with HF severity and predict all-cause and cardiovascular mortality [41, 42]. Beyond potential cardio-renal interactions, studies propose that the mechanism by which plasma β2M affects the heart involves mechanical stretch and induction of inflammation, contributing to the progression of cardiac fibrosis [43, 44], although further research is needed to fully elucidate these pathways.

The diagnostic and prognostic roles of cardiac troponins in cardiac amyloidosis have been extensively validated and are integrated into multiparametric staging systems [8–10, 16, 45]. Additionally, cardiac troponins are helpful in monitoring chemotherapy response in AL amyloidosis and risk stratification of early death following ASCT [16, 46]. In our study, troponin was not included in the LR model's best predictor cohort, but it ranked 7th in the RF model and 5th in the XGBoost model's feature importance rankings, indicating its significance as a predictive factor. In our cohort, an elevation of cTnI was uncommon at initial diagnosis of AL amyloidosis but tended to rise during follow-up and showed marked

abnormalities in patients who ultimately died of cardiac causes. Furthermore, our study included cTnI rather than cardiac troponin T, which has been shown to be a better predictor than cTnI [16]. Therefore, we speculate that the LR model did not include cTnI due to potential lagging in predicting cardiac outcomes; however, there is no evidence to support this hypothesis, which requires further investigation.

Additionally, several treatment-related factors that influence prognosis warrant attention. A recent study demonstrated that complete hematologic response to treatment for AL cardiac amyloidosis can lead to improvements in LV myocardial work indices and better outcomes [47]. Our scoring system includes whether a patient has undergone ASCT, which has been shown to be an effective therapy, but only selected patients can undergo this procedure [1, 17, 18]. These findings underscore the critical importance of early diagnosis and the prioritization of managing modifiable risk factors of the cardiac death in the treatment of AL amyloidosis.

Regarding the consideration of NT-proBNP and BNP, we deliberately included both biomarkers as candidate predictors in our modeling process to address ongoing debates about their prognostic utility in cardiac AL amyloidosis. While NT-proBNP is more commonly utilized in staging systems [8, 9], certain frameworks, such as the 2019 Boston University staging system, prioritize BNP [10]. Notably, NT-proBNP exhibits greater susceptibility to confounding by comorbidities prevalent in AL amyloidosis (e.g., atrial fibrillation, renal dysfunction). To objectively resolve this clinical uncertainty, both biomarkers underwent identical variable selection procedures (stepwise regression, LASSO). Across all models, NT-proBNP consistently demonstrated superior predictive performance for cardiac outcomes and was ultimately retained in the final LR model and nomogram, whereas BNP was statistically excluded. This methodology ensured an unbiased evaluation while rigorously mitigating multicollinearity concerns.

Limitations

Firstly, despite integrating a ten-year cohort from Beijing Chaoyang Hospital and a four-year cohort from two additional centers, the rarity and diagnostic complexity of AL amyloidosis limited our final sample size. Secondly, this study did not include CMR and speckle tracking echocardiography due to limited retrospective data, although these modalities have significant clinical value in diagnosing AL amyloidosis. Future investigations should explore their potential in assessing the risk of cardiac death associated with AL amyloidosis. Thirdly, although our expert panel of cardiologists and hematologists meticulously analyzed the causes of death, the possibility of potential misclassification cannot be completely eliminated. Prospective studies with larger sample sizes will be necessary to validate the findings and enhance the model, which is also one of our planned future undertakings.

Conclusions

The prediction model developed in this study exhibits considerable predictive capability and serves as a potent tool for the clinical assessment of the risk of cardiac death in AL amyloidosis, thereby facilitating the early identification of high-risk patients.

Supplementary Information

The online version contains supplementary material available at https://doi.org/10.1186/s40959-025-00342-5.

Supplementary Material 1

Supplementary Material 2

Supplementary Material 3

Supplementary Material 4

Supplementary Material 5

Supplementary Material 6

Supplementary Material 7

Supplementary Material 8

Acknowledgements

None.

Author contributions

N. Pang, H. Chi, A. Liu and XP. Liu: Conceptualization; N. Pang, Y. Tian, H. Chi and S. Wang: Methodology; N. Pang, Y. Tian, X. Fu, F. Pan, X. Li, D. Wang, L. Xu and J. Luo: Investigation and follow-up; N. Pang and S. Wang: Data curation and statistical analysis; N. Pang and S. Wang: Visualization and Validation; N. Pang: Writing- Original draft preparation; A. Liu and XP. Liu: Supervision and Writing-Reviewing and Editing.

Funding

This work was supported by the National Natural Science Foundation of China, Grant/Award Numbers: 82270325.

Data availability

The data that support the findings of this study are available from the corresponding author upon reasonable request.

Declarations

Competing interests

The authors declare no competing interests.

Author details

[1]Department of Cardiology, Heart Center, Beijing Chaoyang Hospital, Capital Medical University, Beijing, China
[2]Department of Hematology, Beijing Chaoyang Hospital, Capital Medical University, Beijing, China
[3]Multiple Myeloma Clinical Research Center of Beijing, Beijing Chaoyang Hospital, Capital Medical University, Beijing, China
[4]Department of Cardiology, First Hospital of Shanxi Medical University, Taiyuan, Shanxi, China
[5]Department of Cardiology, Second Hospital of Shanxi Medical University, Taiyuan, Shanxi, China

[6]The Third Clinical Medical College, Shanxi Medical University, Taiyuan, Shanxi, China
[7]Department of Cardiology, HTRM Cardiovascular Hospital, Dezhou, Shandong, China

Received: 12 October 2024 / Accepted: 23 April 2025
Published online: 15 May 2025

References

1. Sanchorawala V. Systemic light chain amyloidosis. N Engl J Med. 2024;390(24):2295–307. https://doi.org/10.1056/NEJMra2304088.
2. Merlini G, Palladini G. Light chain amyloidosis: the heart of the problem. Haematologica. 2013;98(10):1492–5. https://doi.org/10.3324/haematol.2013.094482.
3. Escher F, Senoner M, Doerler J, et al. When and how do patients with cardiac amyloidosis die? Clin Res Cardiol. 2020;109(1):78–88. https://doi.org/10.1007/s00392-019-01490-2.
4. Muchtar E, Gertz MA, Kumar SK, et al. Improved outcomes for newly diagnosed AL amyloidosis between 2000 and 2014: cracking the glass ceiling of early death. Blood. 2017;129(15):2111–9. https://doi.org/10.1182/blood-2016-11-751628.
5. Barrett CD, Dobos K, Liedtke M, et al. A changing landscape of mortality for systemic light chain amyloidosis. JACC Heart Fail. 2019;7(11):958–66. https://doi.org/10.1016/j.jchf.2019.07.007.
6. Nienhuis HL, Bijzet J, Hazenberg BP. The prevalence and management of systemic amyloidosis in Western countries. Kidney Dis (Basel). 2016;2(1):10–9. https://doi.org/10.1159/000444206.
7. Huang XH, Liu ZH. The clinical presentation and management of systemic Light-Chain amyloidosis in China. Kidney Dis (Basel). 2016;2(1):1–9. https://doi.org/10.1159/000444287.
8. Dispenzieri A, Gertz MA, Kyle RA, et al. Serum cardiac troponins and N-terminal pro-brain natriuretic peptide: a staging system for primary systemic amyloidosis. J Clin Oncol. 2004;22(18):3751–7. https://doi.org/10.1200/JCO.2004.03.029.
9. Kumar S, Dispenzieri A, Lacy MQ, et al. Revised prognostic staging system for light chain amyloidosis incorporating cardiac biomarkers and serum free light chain measurements. J Clin Oncol. 2012;30(9):989–95. https://doi.org/10.1200/JCO.2011.38.5724.
10. Lilleness B, Ruberg FL, Mussinelli R, et al. Development and validation of a survival staging system incorporating BNP in patients with light chain amyloidosis. Blood. 2019;133(3):215–23. https://doi.org/10.1182/blood-2018-06-858951.
11. Ríos-Tamayo R, Lecumberri R, Cibeira MT, et al. A simple frailty score predicts survival and early mortality in systemic AL amyloidosis. Cancers (Basel). 2024;16(9):1689. https://doi.org/10.3390/cancers16091689.
12. Xing Y, Li X, Zhao J, et al. Advancing precision medicine in Immunoglobulin light-chain amyloidosis: a novel prognostic model incorporating multi-organ indicators. Intern Emerg Med. 2024 May;14. https://doi.org/10.1007/s11739-024-03621-8.
13. Palladini G, Hegenbart U, Milani P, et al. A staging system for renal outcome and early markers of renal response to chemotherapy in AL amyloidosis. Blood. 2014;124(15):2325–32. https://doi.org/10.1182/blood-2014-04-570010.
14. Khwaja J, Ravichandran S, Bomsztyk J, et al. Limited utility of Mayo 2012 cardiac staging system for risk stratification of patients with advanced cardiac AL amyloidosis - analysis of a uniformly treated cohort of 1,275 patients. Haematologica. 2024;109(5):1598–602. https://doi.org/10.3324/haematol.2023.284348.
15. Wechalekar AD, Fontana M, Quarta CC, et al. AL amyloidosis for cardiologists: awareness, diagnosis, and future prospects: JACC: cardiooncology State-of-the-Art review. JACC CardioOncol. 2022;4(4):427–41. https://doi.org/10.1016/j.jaccao.2022.08.009.
16. De Michieli L, Cipriani A, Iliceto S, et al. Cardiac troponin in patients with light chain and transthyretin cardiac amyloidosis: JACC: cardiooncology State-of-the-Art review. JACC CardioOncol. 2024;6(1):1–15. https://doi.org/10.1016/j.jaccao.2023.12.006.
17. Writing C, Kittleson MM, Ruberg FL, Ambardekar AV, et al. 2023 ACC expert consensus decision pathway on comprehensive multidisciplinary care for the patient with cardiac amyloidosis: A report of the American college of cardiology solution set oversight committee. J Am Coll Cardiol. 2023;81(11):1076–126. https://doi.org/10.1016/j.jacc.2022.11.022.
18. Shen K, Tian Z, Gao Y, et al. Chinese consensus on the diagnosis and treatment of Immunoglobulin light-chain cardiac amyloidosis. Chin Med J (Engl). 2024;137(2):127–9. https://doi.org/10.1097/CM9.0000000000002961.
19. Staron A, Zheng L, Doros G, et al. Marked progress in AL amyloidosis survival: a 40-year longitudinal natural history study. Blood Cancer J. 2021;11(8):139. https://doi.org/10.1038/s41408-021-00529-w.
20. Kharoubi M, Bodez D, Bézard M, et al. Describing mode of death in three major cardiac amyloidosis subtypes to improve management and survival. Amyloid. 2022;29(2):79–91. https://doi.org/10.1080/13506129.2021.2013193.
21. Wu Y, Pu C, Zhu W, et al. A risk score to diagnose cardiac involvement and provide prognosis information in patients at risk of cardiac Light-Chain amyloidosis. Front Cardiovasc Med. 2022;9:817456. https://doi.org/10.3389/fcvm.2022.817456.
22. Palladini G, Sachchithanantham S, Milani P, et al. A European collaborative study of cyclophosphamide, bortezomib, and dexamethasone in upfront treatment of systemic AL amyloidosis. Blood. 2015;126(5):612–5. https://doi.org/10.1182/blood-2015-01-620302.
23. Kastritis E, Wechalekar AD, Dimopoulos MA, et al. Bortezomib with or without dexamethasone in primary systemic (light chain) amyloidosis. J Clin Oncol. 2010;28(6):1031–7. https://doi.org/10.1200/JCO.2009.23.8220.
24. Venner CP, Lane T, Foard D, et al. Cyclophosphamide, bortezomib, and dexamethasone therapy in AL amyloidosis is associated with high clonal response rates and prolonged progression-free survival. Blood. 2012;119(19):4387–90. https://doi.org/10.1182/blood-2011-10-388462.
25. Kastritis E, Palladini G, Minnema MC, et al. Daratumumab-Based treatment for Immunoglobulin Light-Chain amyloidosis. N Engl J Med. 2021;385(1):46–58. https://doi.org/10.1056/NEJMoa2028631.
26. Sanchorawala V, Sarosiek S, Schulman A, et al. Safety, tolerability, and response rates of daratumumab in relapsed AL amyloidosis: results of a phase 2 study. Blood. 2020;135(18):1541–7. https://doi.org/10.1182/blood.2019004436.
27. Roussel M, Merlini G, Chevret S, et al. A prospective phase 2 trial of daratumumab in patients with previously treated systemic light chain amyloidosis. Blood. 2020;135(18):1531–40. https://doi.org/10.1182/blood.2019004369.
28. Schwotzer R, Manz MG, Pederiva S, et al. Daratumumab for relapsed or refractory AL amyloidosis with high plasma cell burden. Hematol Oncol. 2019;37(5):595–600. https://doi.org/10.1002/hon.267.
29. Chen Z, Shi A, Dong H, et al. Prognostic implications of premature ventricular contractions and non-sustained ventricular tachycardia in light-chain cardiac amyloidosis. Europace. 2024;26(3):euae063. https://doi.org/10.1093/europace/euae063.
30. Larsen BT, Mereuta OM, Dasari S, et al. Correlation of histomorphological pattern of cardiac amyloid deposition with amyloid type: a histological and proteomic analysis of 108 cases. Histopathology. 2016;68(5):648–56. https://doi.org/10.1111/his.12793.
31. Dorbala S, Vangala D, Bruyere J Jr, et al. Coronary microvascular dysfunction is related to abnormalities in myocardial structure and function in cardiac amyloidosis. JACC Heart Fail. 2014;2(4):358–67. https://doi.org/10.1016/j.jchf.2014.03.009.
32. Nguyen HT, Nguyen CTH. Cardiac amyloidosis mimicking acute coronary syndrome: a case report and literature review. Eur Heart J Case Rep. 2020;4(6):1–7. https://doi.org/10.1093/ehjcr/ytaa325.
33. Tsai SB, Seldin DC, Wu H, et al. Myocardial infarction with clean coronaries caused by amyloid light-chain AL amyloidosis: a case report and literature review. Amyloid. 2011;18(3):160–4. https://doi.org/10.3109/13506129.2011.571319.
34. Pagnesi M, Adamo M, Sama IE, et al. Impact of mitral regurgitation in patients with worsening heart failure: insights from BIOSTAT-CHF. Eur J Heart Fail. 2021;23(10):1750–8. https://doi.org/10.1002/ejhf.2276.
35. Heitzinger G, Pavo N, Koschatko S, et al. Contemporary insights into the epidemiology, impact and treatment of secondary tricuspid regurgitation across the heart failure spectrum. Eur J Heart Fail. 2023;25(6):857–67. https://doi.org/10.1002/ejhf.2858.
36. Minga I, Kwak E, Hussain K, et al. Prevalence of valvular heart disease in cardiac amyloidosis and impact on survival. Curr Probl Cardiol. 2024;49(4):102417. https://doi.org/10.1016/j.cpcardiol.2024.102417.
37. Tomasoni D, Aimo A, Porcari A, et al. Prevalence and clinical outcomes of isolated or combined moderate to severe mitral and tricuspid regurgitation in patients with cardiac amyloidosis. Eur Heart J Cardiovasc Imaging. 2024;25(7):1007–17. https://doi.org/10.1093/ehjci/jeae060.
38. Palumbo A, Avet-Loiseau H, Oliva S, et al. Revised international staging system for multiple myeloma: A report from international myeloma working

group. J Clin Oncol. 2015;33(26):2863–9. https://doi.org/10.1200/JCO.2015.61.2267.
39. Royal V, Leung N, Troyanov S, et al. Clinicopathologic predictors of renal outcomes in light chain cast nephropathy: a multicenter retrospective study. Blood. 2020;135(21):1833–46. https://doi.org/10.1182/blood.2019003807.
40. Zhang T, Lin Z, Zheng Z, et al. Prognostic significance of β2-microglobulin decline index in multiple myeloma. Front Oncol. 2024;14:1322680. https://doi.org/10.3389/fonc.2024.1322680.
41. Foster MC, Coresh J, Hsu CY, et al. Serum β-Trace protein and β2-Microglobulin as predictors of ESRD, mortality, and cardiovascular disease in adults with CKD in the chronic renal insufficiency cohort (CRIC) study. Am J Kidney Dis. 2016;68(1):68–76. https://doi.org/10.1053/j.ajkd.2016.01.015.
42. Astor BC, Shafi T, Hoogeveen RC, et al. Novel markers of kidney function as predictors of ESRD, cardiovascular disease, and mortality in the general population. Am J Kidney Dis. 2012;59(5):653–62. https://doi.org/10.1053/j.ajkd.2011.11.042.
43. Hilt ZT, Ture SK, Mohan A, et al. Platelet-derived β2m regulates age related monocyte/macrophage functions. Aging. 2019;11(24):11955–74. https://doi.org/10.18632/aging.102520.
44. Li Y, Zhang X, Li L, et al. Mechanical stresses induce paracrine β-2 microglobulin from cardiomyocytes to activate cardiac fibroblasts through epidermal growth factor receptor. Clin Sci (Lond). 2018;132(16):1855–74. https://doi.org/10.1042/CS20180486.
45. Vergaro G, Castiglione V, Aimo A, et al. N-terminal pro-B-type natriuretic peptide and high-sensitivity troponin T hold diagnostic value in cardiac amyloidosis. Eur J Heart Fail. 2023;25(3):335–46. https://doi.org/10.1002/ejhf.2769.
46. Muchtar E, Dispenzieri A, Wisniowski B, et al. Graded cardiac response criteria for patients with systemic light chain amyloidosis. J Clin Oncol. 2023;41(7):1393–403. https://doi.org/10.1200/JCO.22.00643.
47. Briasoulis A, Bampatsias D, Petropoulos I, et al. Left ventricular myocardial work improves in response to treatment and is associated with survival among patients with light chain cardiac amyloidosis. Eur Heart J Cardiovasc Imaging. 2024;25(5):698–707. https://doi.org/10.1093/ehjci/jead351.

Publisher's note